Wallops' Low Elevation Link Analysis for the Constellation Launch/Ascent Links

Kar-Ming Cheung, Christian Ho,
Anil Kantak, Charles Lee
Jet Propulsion Laboratory, California Institute of Technology
4800 Oak Grove Drive
Pasadena, CA 91109
818-393-0662
Kar-Ming.Cheung@jpl.nasa.gov, Christian.Ho@jpl.nasa.gov,
Anil.Kantak@jpl.nasa.gov, Charles.H.Lee@jpl.nasa.gov

Robert Tye, Edger Richards, and Team
NASA Wallops Flight Facility
34200 Fulton Street
Wallops, VA 23337
Rob.Tye@nasa.gov, Edgar.Richards@ljtinc.com

Catherine Sham, Adam Schlesinger, and Team
NASA Johnson Space Center
2101 NASA Parkway
Houston, TX 77058
Catherine.C.Sham@nasa.gov, Adam.A.Schlesinger@nasa.gov

Brian Barritt and Team
NASA Glenn Research Center
21000 Brookpark Road
Cleveland, OH 44135
Brian.Barritt@nasa.gov

Abstract[1 2 3] - Prior to the redirection of the Constellation Program, the Wallops 11.3-meter ground station was tasked to support the Orion's Dissimilar Voice (DV) link and the Ares's Development Flight Instrument (DFI) link. Detailed analysis of the launch trajectories indicates that during the launch and ascent operation, the critical events of Orion-Ares main engine cut off (MECO) and Separation occur at low elevation angle. We worked with engineers from both Wallops Flight Facility (WFF) and Johnson Space Center (JSC) to perform an intensive measurement and link analysis campaign on the DV and DFI links. The main results were as follows:

(1) The DV links have more than 3 dB margin at MECO and Separation.

(2) The DFI links have 0 dB margin at Separation during certain weather condition in summer season.

(3) Tropospheric scintillation loss is the major impairment at low elevation angle.

(4) The current scintillation models in the Recommendation ITU-R P.618 (Propagation data and prediction methods required for the design of Earth-space telecommunication systems), which are based on limited experimental and theoretical work, exhibit idiosyncratic behaviors. We developed an improved model based on the measurements of recent Shuttle mission launch and ascent links and the ITU propagation data.

(5) Due to the attitude uncertainty of the Orion-Ares stack, the high dynamics of the launch and ascent trajectory, and the irregularity of the Orion and Ares antenna patterns, we employed new link analysis approach to model the spacecraft antenna gain.

In this paper we discuss the details of the aforementioned results.

TABLE OF CONTENTS

2 IEEEAC paper #0012, Version 1, Updated March 24, 2010.

3 This work was performed at the Jet Propulsion Laboratory, California Institute of Technology, under a contract with the National Aeronautics and Space Administration.

1. INTRODUCTION

In January 2004, President George W. Bush initiated the new Vision for Space Exploration for NASA. The fundamental goal of this vision was to advance U.S. scientific, security and economic interests through a robust space exploration program, which included sustained and affordable human and robotic program to explore the solar system and beyond. To execute this goal, the human spaceflight program, known as the Constellation Program (CxP), was formed to build the next generation spacecraft Orion and launch vehicle, Ares, in order to transport human and cargo to International Space Station (ISS), moon, and Mars. To support the frequent launches of the Constellation missions, CxP will rely on the Space Communication and Navigation (SCaN) organization to support the Orion and Ares communications and tracking needs during the launch and ascent phase, particularly on the Orion's Dissimilar Voice (DV) link and the Ares's Developmental Flight Instrument (DFI) link. The Orion's DV link provides an independent 2-way voice service system to bridge the gaps in primary voice service caused by expected dropout to maximize successful voice communication during the dynamic event of launch and ascent. The Ares' DFI link provides a 20 Mbps downlink telemetry to collect the thermal, acceleration, acoustics, vibration, and other senor measurements during Ares' launch and ascent operations. This paper focuses on the detailed link analysis and challenges of using the SCaN's Wallops 11.3-meter ground station to support the Orion's DV link and the Ares's DFI link.

An important consideration for SCaN's support of CxP's DV and DFI links is to ensure that there would be sufficient link margins to close the links during the critical events of Main Engine Cut Off (MECO) and Separation during the launch and ascent phase. Preliminary coverage analysis indicates that for many CxP launch trajectories the Wallops ground station would be tracking the Orion and Ares at an elevation angle much lower than 5-degree during the MECO and Separation events, during which the unpredictable weather and propagation effects might impair the links. If Wallops Station is found to be insufficient to track the CxP DV and DFI links, SCaN would have to build a new ground station in New Hampshire to fill this gap.

In September 2009, the Network Integration and Engineering (NI&E) Project of SCaN launched a vigorous measurement and link analysis campaign on the DV and DFI links. This study involved engineers from Jet Propulsion Laboratory, Goddard's Wallops Flight Facility, Johnson Space Center, and Glenn Research Center:

(1) JPL was primarily responsible for the link analysis and development of low elevation link models.

(2) Goddard's WFF was primarily responsible for the low elevation WFF antenna G and T measurements.

(3) JSC provided Orion's trajectory, attitude, and link parameters to support the link analysis.

(4) GRC used independent COTS tool (STK) to crosscheck with JPL's link analysis, and to provide visualization of Orion and Ares trajectories, attitude, and antenna pointing.

The rest of the paper is organized as follows: Section 2 provides the characteristics of the Orion-Ares launch and ascent links. Section 3 describes the analysis results. Section 4 discusses the highlights and challenges of the study. Section 5 discusses a number of follow-on studies, and Section 6 provides the concluding remarks.

2. CHARACTERISTICS OF THE ORION-ARES LAUNCH AND ASCENT LINKS

In this section, we discuss the key components of the Orion-Ares launch and ascent links. This includes the launch and ascent trajectory profiles, the launch attitude, and the spacecraft and ground station link parameters used in the link calculations.

Orion-Ares' Launch Trajectory Profiles and Attitude

There are two types of Orion-Ares trajectories; one goes to the International Space Station (ISS), which typically would ascend into further northern latitudes and the other goes to the Moon whose orbit trajectory is not inclined as much. Figure 1 provides the proper perspectives of the launch and ascent footprints on Earth of both types of trajectories. There are seven flight paths superimposed on the two-dimensional map of Earth with four trajectories (TD7-B, TD7-I, TD7-J, TD7-K) going to the Moon and three (TD7-E, TD7-F, TD7-G) going to the ISS. The elevation angles and ranges from the Wallops stations are displayed in Figure 2 Figure 3.

In our analysis, we will focus on the trajectories that go to the ISS, namely the TD7-E, F, and G trajectories. Once launched from Kennedy Space Center, the Orion-Ares stack cruises along the northeastern coast of the Continental United States. For a typical launch, the spacecraft is in view with the 10.3 m ground antenna at the Wallops Flight Facility (WFF) at approximately 150 seconds after launch, when the range is about 1,100 km. As the spacecraft cruises along the coast, the spacecraft comes closer to Wallops and then goes away. Orion's attitudes during its contact with Wallops are very much constant with no major rotation or spinning.

The closest range between Orion and Wallops during the launch and ascent phase is roughly 500 km, and the highest horizon elevation to the spacecraft at Wallops is around 15 degrees. The spacecraft's MECO and Separation events are at about 560 seconds and 590 seconds after launch, respectively.

Though Wallops remains in view with the spacecraft during these important maneuvers, the elevation between Wallops and the spacecraft is at a low elevation angle between 3 to 7 degrees. Moreover, at such instances, Wallops appears to be looking at the tail of the Orion spacecraft, where the nulls of the antenna patterns are, and the gain pattern is significantly affected by the vehicle structure. Also, a large portion of the trajectory path will be over the Atlantic Ocean. It is expected that atmospheric loss and scintillation loss at low elevation angles will play an essential role and could impair the RF communications between the spacecraft and the ground station.

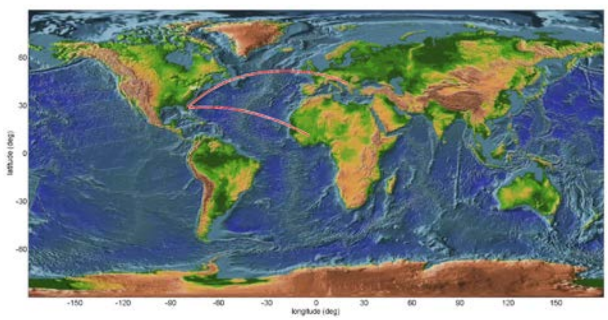

Figure 1 - Ares Launch and Ascent Flight Paths to the ISS (upper path) and to the Moon (lower path

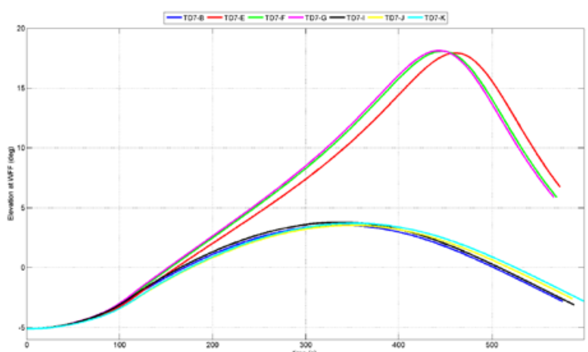

Figure 2 – Elevation Angle Profiles of Orion as Viewed by Wallops during Launches and Ascents to the ISS (TD7-E, TD7-F, TD7-G) and to the Moon (TD7-B, TD7-I, TD7-J, TD7-K)

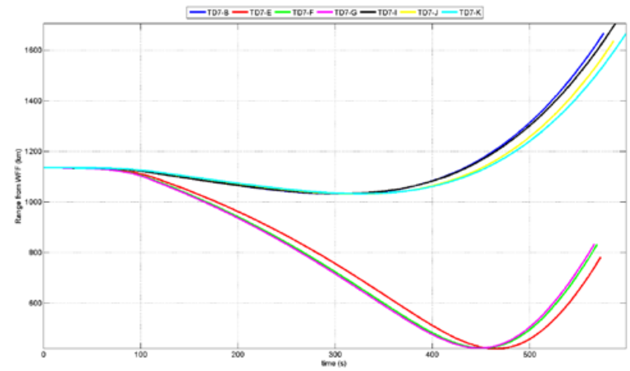

Figure 3 – Range Profiles of Orion from Wallops during Launches and Ascents to the ISS (TD7-E, TD7-F, TD7-G) and to the Moon (TD7-B, TD7-I, TD7-J, TD7-K)

Description of DV and DFI Link Parameters

The DV and DFI link parameters are summarized in the following tables: Table 1 and Table 2 give the values for the Orion to Wallops DV downlink parameters and Ares to Wallops DFI downlink parameters respectively. Table 3 provides the values for the Wallops to Orion's uplink parameters.

Table 1. Orion to Wallops DV Downlink Parameters

Transmitter Frequency	2370 (MHz) (S-Band)
Data Rate	10.24 kbps
Bit Error Rate	10^{-8}
Modulation Format	NRZ-L Bits, SQPSK Suppressed Carrier Modulation
DV Transmitter Power	8 W
Antenna Circuit Loss	1.5 dB
Antenna pointing Loss	0 dB (Very low gain antenna)
Orion Antenna Gain	Since the link budget will track the trajectory, Orion antenna gain will be a variable depending upon the attitude of the Ares - Orion. Minimum: -22.0 dB Maximum: 2.3 dB
Range	Since the link budget will track the trajectory, Orion antenna gain will be a

	variable depending upon the position of Ares – Orion in its launch orbit. First Visible: 1029 km Minimum Distance: 480 km. Maximum: 1331 km
Wallops Antenna elevation Angle	Since the link budget will track the trajectory, Wallops Ground Station antenna elevation angle will be a variable depending upon the position of Ares – Orion in its launch orbit. Minimum: 0 Deg Maximum: 15 Deg
Wallops Antenna Particulars	Diameter: 11.3 (m); Gain: 46.3 dB
Antenna pointing Loss	0.15 dB
Gain/Noise Temp	22.1 dB/K
Weather Conditions At Launch	Temp: 0 Deg; RH: 0.3; Rain Rate: 10 mm/Hr P Factor: 1% and 5%
Downlink Coding Used	Uncoded
Required Eb/No	11.97 to achieve 10^{-8} BER
Receiver Losses	3 dB (Assumed)

Table 2. Ares to Wallops DFI Downlink Parameters

Transmitter Frequency	2370 (MHz) (S-Band)
Data Rate	20 Mbps (HDR)
Bit Error Rate	10^{-8}
Modulation Format	NRZ-L Bits, SQPSK Suppressed Carrier Modulation
DFI Transmitter Power	50 W
Antenna Circuit Loss	1.5 dB
Antenna pointing Loss	0 dB (Very low gain antenna)
Orion Antenna Gain	Since the link budget will track the trajectory, Orion antenna gain will be a variable depending upon the attitude of the Ares - Orion. Minimum: -22.0 dB Maximum: 4.8 dB
Range	Since the link budget will track the trajectory, Orion antenna gain will be a variable depending upon the position of Ares – Orion in its launch orbit. First Visible: 1029 km Minimum Distance: 480 km. Maximum: 1331 km
Wallops Antenna elevation Angle	Since the link budget will track the trajectory, Wallops Ground Station antenna elevation angle will be a variable depending upon the position of Ares – Orion in its launch orbit. Minimum: 0 Deg Maximum: 15 Deg
Wallops Antenna Particulars	Diameter: 11.3 (m); Gain: 46.3 dB
Antenna pointing Loss	0.15 dB
Gain/Noise Temp	22.1 dB/K
Weather Conditions At Launch	Temp: 0 Deg; RH: 0.3; Rain Rate: 10 mm/Hr P Factor: 1% and 5%
Downlink Coding Used	Uncoded
Required Eb/No	11.97 to achieve 10^{-8} BER

Table 3. Wallops to Ares – Orion Uplink Parameters

Transmitter Frequency	2370 (MHz) (S-Band)
Data Rate	10.24 kbps
Bit Error Rate	10^{-8}
Modulation Format	NRZ-L Bits, BPSK Suppressed Carrier Modulation
Transmitter Power	100 W
Antenna Circuit Loss	1.0 dB
Antenna pointing Loss	0 dB
Orion Antenna Gain	Since the link budget will track the trajectory, Orion antenna gain will be a variable depending upon the attitude of the Ares - Orion. Minimum: -27.0 dB Maximum: 2.5 dB
Range	Since the link budget will track the trajectory, Orion antenna gain will be a variable depending upon the position of Ares – Orion in its launch orbit. First Visible: 1029 km Minimum Distance: 480 km. Maximum: 1331 km
Wallops Antenna elevation Angle	Since the link budget will track the trajectory, Wallops Ground Station antenna elevation angle will be a variable depending upon the position of Ares – Orion in its launch orbit. Minimum: 0 Deg Maximum: 15 Deg
Wallops Antenna Particulars	Diameter: 11.3 (m); Gain: 46.3 dB
Antenna pointing Loss	0.15 dB
Weather Conditions At Launch	Temp: 0 Deg; RH: 0.3; Rain Rate: 10 mm/Hr P Factor: 1% and 5%
Uplink Coding Used	Uncoded
Required Eb/No	11.97 to achieve 10^{-8} BER
Receiver Losses	3 dB (Assumed)

3. Link Analysis Results

It should be noted that only the DV channel has both uplink and downlink while the DFI has only downlink. Using the parameters given in Tables 1, 2, and 3 appropriate link budgets were run with the standard Consultative Committee on Space Data System (CCSDS) design control table and results were plotted in the following six figures.

Figures 4, 5, and 6 show the downlink data margins for the DFI and DV links for trajectories TD7-E, F and G respectively. Similarly Figures 7, 8, and 9 show the uplink data margins for DV links for the same shuttle trajectories. Each figure also shows the ground station antenna true elevation angle and the apparent elevation angle curves for the trajectory used for the downlink link budget. Also each of the three figures shows the critical events of the MECO and Separation so that the link margins at those critical events can be evaluated.

The link calculations include the effects of weather degradation as well as the scintillation loss predicted by the ITU-R P.618 models. The percentage of time the degradation is above a certain loss as predicted by the scintillation model is denoted by *'p'*. The link margin curves corresponding to p = 1% and p = 5% are included in the each of the figures. Another parameter required in the computation of the low elevation angle scintillation loss that needs to be inserted in the link calculations is the ratio of land coverage to ocean coverage, and considering the North-Eastern trajectory from Florida it is assumed to be 80%.

These figures indicate that at all critical points of the trajectory, i.e., between the start of MECO and end of Separation, the data margins of all DV links are above 3 dB. Figure 5, and Figure 6 indicate that for some comparatively small regions of time (the x axis parameter for the graphs) the DFI links yield data margin below 3 dB at separation event for the case of p=1%.

All the deterministic link effects such as the range increase at the horizon of the tracking station and the high data rate of the DFI link are assumed to be taken into account in the link design and are not contributing factors in having the link margin below 3 dB for the DFI link. There are, however, two distinct link loss mechanisms that are random in nature and cannot be predicted. First, the atmospheric attenuation of the link that is a function of atmospheric humidity, atmospheric pressure and moisture content of the atmosphere and rain along with the elevation angle at the tracking station can be substantial depending upon the weather conditions. This loss is estimated using the techniques described in references [1] – [5]. The second loss that is random is the low elevation angle scintillation loss that is present especially when the separation event starts. For the particular case of the DFI links in Figures 4 and 5, the combined effect of these two losses seems to have resulted in lowering of the margin below 3 dB. For these links even if the DFI data margin does go below 3 dB, it is true for p = 1% case that happens only rarely and time interval for which the margin is below 3 dB is small in extent. Also it should be remembered that the data margin does go below 3 dB for those links. However, the margin never goes below 0 dB for the entire track, indicating that the received data will still have the desired purity (Bit Error Rate), but without any margin.

Figure 7,Figure 8, and Figure 9 show the DV uplink data margins for trajectories TD7-E, F, and G respectively. These figures indicate that for uplink, between the start of MECO and the end of Separation, the data margins of the DV uplink links are way above 3 dB.

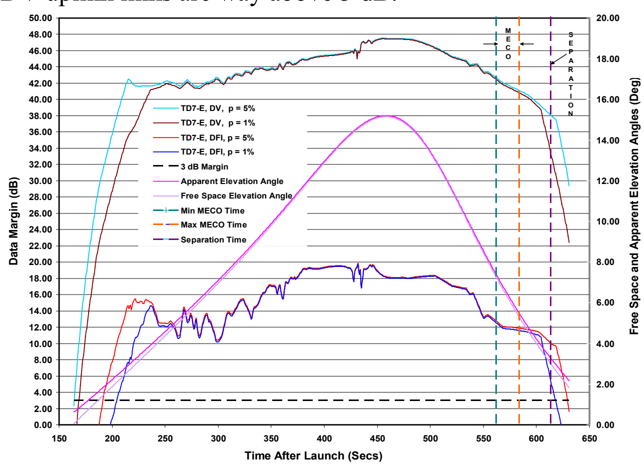

Figure 4 - Data margins for DFI and DV downlinks for trajectory TD 7-E

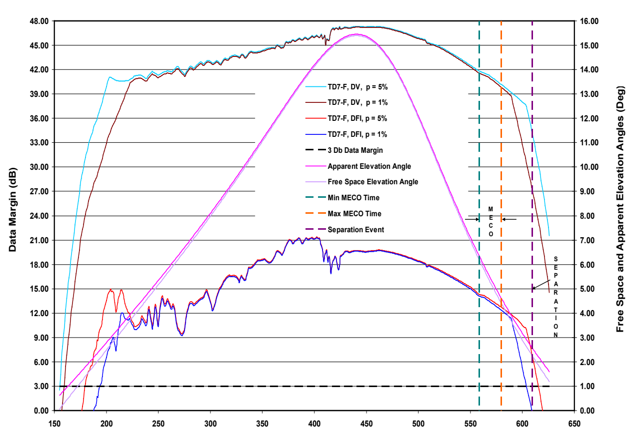

Figure 5 - Data margins for DFI and DV downlinks for trajectory TD 7-F

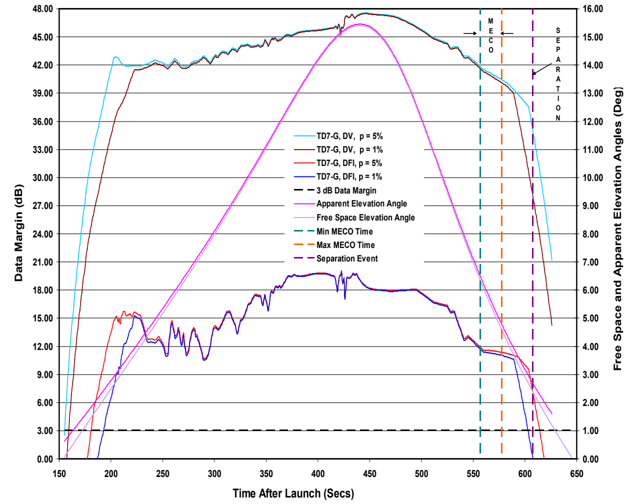

Figure 6 - Data margins for DFI and DV downlinks for trajectory TD 7-G

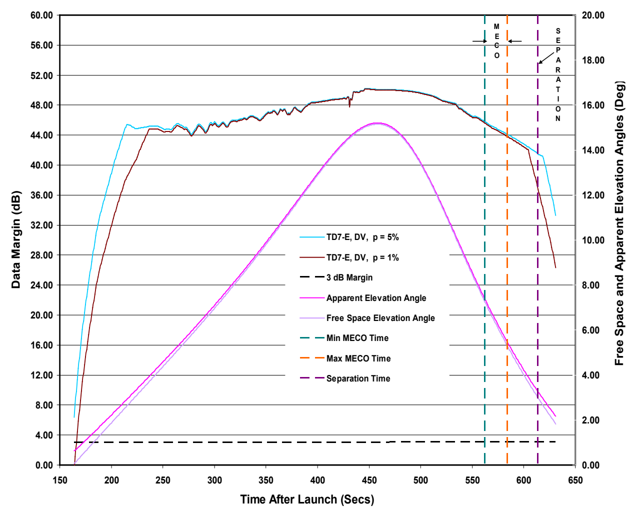

Figure 7 - Data margin for DV uplinks for trajectory TD 7-E

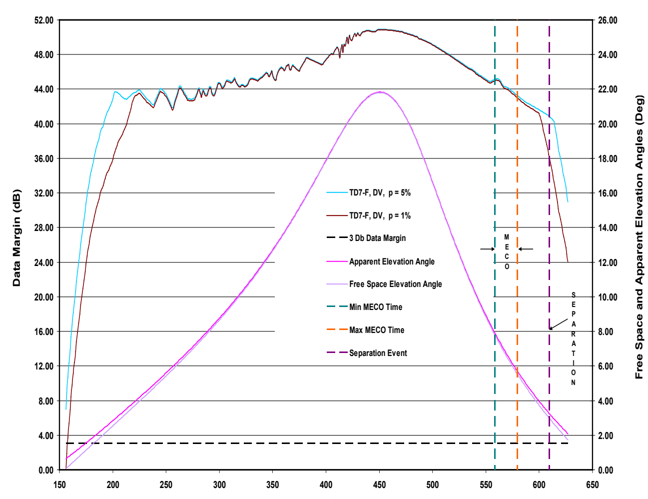

Figure 8 - Data margin for DV uplinks for trajectory TD 7-F

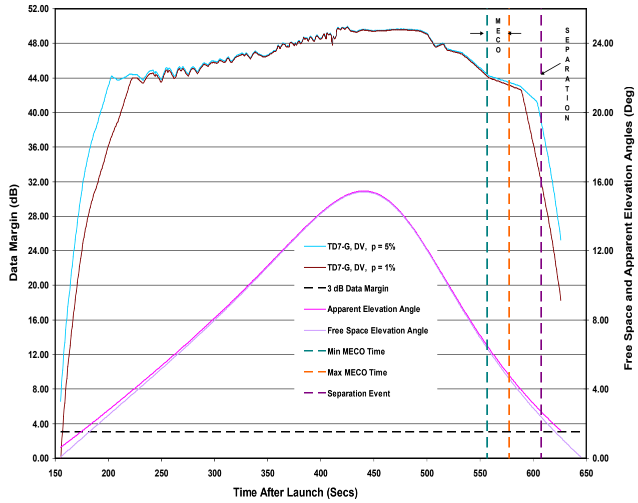

Figure 9 - Data margin for DV uplinks for trajectory TD 7-G

4. Highlights and Challenges of the Study

As with any study, the team faced a number of challenges that had to be overcome to achieve successful results. This section discusses some of these challenges and outlines the mitigation methods employed.

Wallops' Low Elevation Measurements

The Wallops low elevation test involved measuring the S-band Gain over Temperature (G/T) of the Wallops Island, VA. 11.3 Meter antenna. The test was performed using the Y-Factor method and repeated at different cold sky elevation angles. The Y-Factor is used to determine the ratio of power received by the antenna first when pointed at a reference radio star with a known flux density (or hot sky) and then repositioned to the quiet or cold sky. The quiet sky is an area of the sky where there is little or no known radiators in the spectrum of interest.

The resultant G/T characterizes the antenna performance or figure of merit. At low elevations, this figure of merit is progressively degraded by increased thermal noise from the earth's surface and increased attenuation due to additional atmospheric effects. The degraded G/T measurement at low elevation angles is especially important to fully understand the expected data degradation that will be encountered as the spacecraft is tracked through this low trajectory.

The Sun was selected as a hot sky noise source to measure the antennas G/T. While the sun is not a point source, it is the strongest celestial source of electromagnetic radiation in S-Band. The sun subtends a relatively large arc angle of 0.5 degrees, so the flux variations across the antennas 0.8 degrees beam width were compensated with a beam width correction factor.

At higher elevation angles (≥ 5º) where the majority of a spacecraft tracking occurs, the G/T measurement served as the baseline for the overall antenna performance. After a successful high elevation angle measurement, the antenna elevation was lowered to 5º, 4º, 3º, 2º, 1º, and 0º and the G/T measurements were repeated. A cold sky power measurement was recorded for each elevation angle and used to compute the estimated G/T degradation. A manual technique of measuring the hot and cold Y-factor data with a spectrum analyzer was implemented with measurements made at the base of the antenna at the output of the down converter in order to provide high accuracy measurements. Examples of cold sky, Y-factor, and G/T measurements are given in Table 4.

For the communication links themselves, tropospheric scintillation, the rapid variation in a signal's amplitude and phase resulting from the changing refractive index of the earth's atmosphere, is the dominant impairment to CxP's DV and DFI links at low elevation angles and was another challenge that the team faced in this study. Unfortunately, existing ITU-R models used to estimate the tropospheric scintillation effects are based on limited experimental and theoretical work and can therefore be problematic. Analysis of Space Shuttle or other launch vehicles with similar communication data would provide more accurate link analysis for the DV and DFI links. Additional investigation was performed using the Space Shuttle S-band tracking data from the Wallops 11 meter and Merritt Island Launch Annex (MILA) 9 meter antennas starting with the STS-130 mission in February 2010. This assisted in the determination that the current ITU-R model contained errors. The results from this additional testing assisted in advancing the state-of-the-art modeling the tropospheric scintillation loss.

Table 4. WGS 11M Measured G/T between Azimuth 50º - 55º and Elev 5º - 0º

Cold Sky Measurements (dBm)						
True Azimuth Angle	**50**	**51**	**52**	**53**	**54**	**55**
Antenna Angle	**230**	**231**	**232**	**233**	**234**	**235**
5º Elevation	-110.3	-110.3	-110.3	-110.3	-110.3	-110.4
4º Elevation	-110.1	-110.1	-110.1	-110.1	-110.1	-110.4
3º Elevation	-109.8	-109.8	-109.8	-109.8	-109.8	-109.8
2º Elevation	-109.8	-109.8	-109.8	-109.8	-109.8	-109.7
1º Elevation	-109.3	-109.3	-109.3	-109.3	-109.3	-109.4
0º Elevation	-107.8	-107.8	-107.8	-107.8	-107.8	-108.5

Y Factor, Hot Sky = -91.6 dBm						
True Azimuth Angle	**50**	**51**	**52**	**53**	**54**	**55**
Antenna Angle	**230**	**231**	**232**	**233**	**234**	**235**
5º Elevation	18.7	18.7	18.7	18.7	18.7	18.8
4º Elevation	18.5	18.5	18.5	18.5	18.5	18.8
3º Elevation	18.2	18.2	18.2	18.2	18.2	18.2
2º Elevation	18.2	18.2	18.2	18.2	18.2	18.1
1º Elevation	17.7	17.7	17.7	17.7	17.7	17.8
0º Elevation	16.2	16.2	16.2	16.2	16.2	16.9
G/T (dB/K), Sag Hill Solar Radio Flux Values (1/15/2010) 1415 MHz = 67, 2695 MHz = 98						
True Azimuth Angle	**50**	**51**	**52**	**53**	**54**	**55**
Antenna Angle	**230**	**231**	**232**	**233**	**234**	**235**
5º Elevation	23.23	23.23	23.23	23.23	23.23	23.33
4º Elevation	23.02	23.02	23.02	23.02	23.02	23.33
3º Elevation	22.72	22.72	22.72	22.72	22.72	22.72
2º Elevation	22.72	22.72	22.72	22.72	22.72	22.62
1º Elevation	22.21	22.21	22.21	22.21	22.21	22.31
0º Elevation	20.68	20.68	20.68	20.68	20.68	21.40

Idiosyncrasies of ITU-R trophospheric scintillation model and Interaction with US Study Group 3

Physics Behind the ITU Scintillation Model—At low elevation angle, the most dominant propagation loss is due to the tropospheric scintillation and multipaths. Below 5° elevation, scintillation loss drastically increases with decreasing elevation angle. For example, at 2° elevation, the total losses as a result of gaseous, cloud, and rain are only a few dB, whereas scintillation loss can be over 16 dB at 1% of time.

The main cause of tropospheric scintillation loss is the turbulent layer and the irregularity of refractive index through the lower atmosphere. Above the ocean surface, there are usually thicker turbulent layer and sharper refractivity gradients, thus, resulting in larger scintillation loss. The scintillation loss usually increases with increasing signal frequency, longer path length, decreasing receiving antenna size, and decreasing percentage of time. At very low elevation angle the tropospheric scintillation loss, which is due to turbulent layer and sharp refractivity index gradients, and multipath loss, which is due to the radio paths through the different air parcels, are almost indistinguishable. This is why the ITU model (documented in ITU-R P.618) includes both fading phenomena at elevation angles less than 5°.

At low elevation angles, the ionospheric scintillation loss on the S-band radio wave propagation is almost negligible at middle latitude region such as Wallops. To calculate the propagation loss, a flat Earth model does not apply, because $L_q = L_{90}(dB)/\sin\theta$ is only good for $5° < \theta < 90°$, where L_{90} is the zenith loss for gaseous absorption, cloud and rain scattering (not include the scintillation), and θ is the apparent elevation angle.

To calculate the loss along a low elevation path, we should use a round Earth model:

$$L_q = L_{90}(dB)\left\{\left[(a+h)^2 - a_e^2\cos^2\theta\right]^{1/2} - a_e\sin\theta\right\}/h \qquad (1)$$

where a_e is the effective earth radius, and h is the satellite height.

Figure 10 and Table 5 show the propagation losses for a case at Wallops. Table 6 shows the Radio-Climatic Parameters at Wallops used in the propagation loss calculations.

Current ITU Scintillation Model Standard and its Idiosyncrasies—There were relatively very fewer experiment results for low elevation angle scintillation. ITU recommendation (P.618-10) discusses three scintillation models for low elevation angle scenarios:

Section 2.4.1: amplitude scintillation for > 4° elevation angle (which is mainly based on Karasawa model, here we call it as the normal fading model)

Section 2.4.2: deep fading of scintillation/multipath for < 5° elevation angle

Section 2.4.3: shallow fading of scintillation/multipath for < 5° elevation angle

The normal fading model defined in Section 2.4.1 is recommended to evaluate the scintillation loss for higher elevation angles (from 90° zenith to as low as 4°).

The scintillation loss for the time percentage p is given by

$$A_s(p) = a(p).\sigma \qquad (2)$$

where the time percentage factor *a(p)* is expressed as

$$a(p) = -0.061(\log_{10} p)^3 + 0.072(\log_{10} p)^2 - 1.71(\log_{10} p) + 3.0 \qquad (3)$$

and the standard deviation of the signal fading σ is given by

$$\sigma = \sigma_{ref} f^{7/12} g(x) / (\sin\theta)^{1.2} \qquad (4)$$

where σ_{ref} is the referenced standard deviation in dB (defined in equation 27 in Recommendation ITU-R P.618), *f* is signal frequency in GHz, and *g(x)* is the antenna average factor defined in equation (30) in ITU-R P.618. The model is good for a frequency range of 4 to 20 GHz, 0.01 to 50% of time and for above 4° elevation angle. Figure 10 shows scintillation loss for elevation angle 4° and above for various percentages at Wallops.

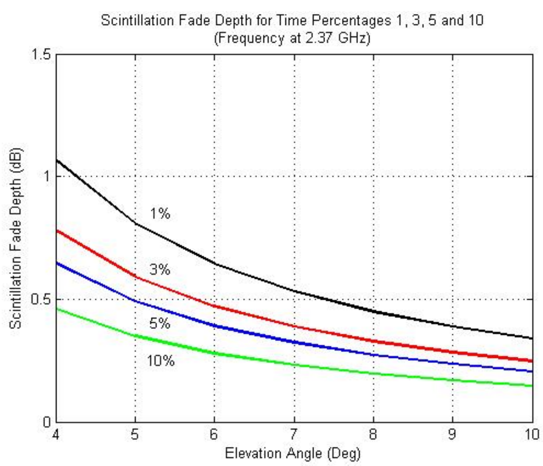

Figure 10- Scintillation Loss for Low Elevation Angles for Various % Based on Models in ITU-R P.618, Section 2.4.1

Deep fading frequently occurs for a radio path over a large water surface with a low path height.

For the Wallops site, the ground station tracks a spacecraft launch that is typically rising from the southwest direction and setting in the northeast direction. During the flight the radio path traverses a significant portion above the ocean. This increases the geoclimatic factor K_w, which in turn increases the scintillation loss.

As defined in equation 34 in ITU-R P.618, the geoclimatic factor K_w is a function of P_L and C_0, where P_L is the percentage of time that the refractivity gradient in the lowest 100 m of the atmosphere is less than -100 N unite/km, and C0 is 76 +6*r* (*r* is the fraction of the propagation path over the water). For a typical Wallops link path, we have $r = 0.9$.

At four seasons, we have:

P_L= 4 (%) in February; P_L= 10 (%) in May;

P_L= 15 (%) in August; P_L= 7 (%) in November;

The deep fading depth A_{ref} (in dB) exceeded for a percentage *p* is given by

$$A_{ref} = 10\log K_w + 9\log f - 55\log(1+\theta) - 10\log p \qquad (5)$$

where θ is the apparent elevation angle in mrad. This model is only good for A_{ref} >25 dB, frequency between 1 and 45 GHz, and elevation angle from 0.5° to 5°.

For the scintillation loss less than 25 dB, ITU-R P.618 suggests to use the shallow fading model defined in Section 2.4.3. However, we find the recommended techniques fail to converge to a meaningful solution in some cases. This iteration technique recommended in the section is complicated and is hard to use. When we apply the model, we often see that the criteria q_t< 0 does not meet, thus there is no solution, even we increase the A_t to 35 dB as suggested in Step 6 in this section. Most importantly, loss values calculated from the shallow fading model have large discrepancies when compared with loss values calculated from the normal model in the elevation angle range between 4° and 5°. We found that the discontinuity for loss solution to be clearly showed in the AGI's STK software when the link analysis is performed at low elevation angles.

Thus the existing ITU-R scintillation models do not guarantee a valid solution for scintillation loss over the low elevation angle range. To solve this problem, we developed new interpolation techniques to formulate models that bridge the gaps for the loss calculation in this overlapping region. Another issue is that both models cover different percentage range (Shallow model for *p*% <63% while normal model for *p*%<50%). Thus we need to develop new modeling techniques that provide smooth transition between the three piece-wise scintillation models, namely the normal, shallow, and deep fading models, for all ranges of elevation angles and percentages.

Interaction with the ITU Propagation Study Group—We have discussed the aforementioned modeling problems with the ITU US Study Group 3, and got the support from the chairman Mr. Paul McKenna to develop new mathematical techniques and to use new empirical data to improve the low elevation angle scintillation model. The details are discussed in the next section. Since May 2010, we have joined the US SG3 monthly meeting to report our progress in this task. We are in the process of drafting a new ITU recommendation to replace the old Section 2.4.3 in ITU-R P.618. It will be submit to this year SG3 meeting soon.

Table 5. Propagation Loss for Low Elevation Links between Wallops 11m Station and TR-7 at 2.37GHz

Link Scenario #	Time sec	AZ deg	Elevation Angle (degree)	Distance (km)	Free Space Loss (dB)	Gaseous Absorption (H_2O= 12 g/m^3)	Rain Attenuation at 1.0% of Time	Cloud Attenuation at 1.0% of Time	Scintillation /Multipath at 1.0% of Time	Total Propagation Loss (dB)	Notes
1	594	73.7	5.69	845.65	158.48	0.30	0.09	0.01	0.92	159.80	MECO
2	599	72.0	5.23	879.01	158.82	0.33	0.10	0.01	1.02	160.28	physical mask at WLP
3	613	69.8	4.03	971.58	159.69	0.43	0.13	0.01	3.89	164.15	
4	624	68.0	3.17	1046.18	160.33	0.54	0.16	0.02	7.93	168.98	MECO+30s

Notes:

- We have used the following ITU-R model for this propagation loss calculation: Recommendation ITU-R P676, P.453, P.618, P.836, P.834, P.836, P.838, and P.840, etc. [6] – [12]
- We have used the following parameters for this calculation at Wallops: refractive index=360N, refractive gradient=50N, water vapor density=12 g/m^3, rainfall rate at 1.0% of time = 2.5mm/h, and cloud liquid water content at 1.0% of time =1.2 kg/m^2.
- Propagation losses due to rain attenuation, cloud attenuation, and scintillation/multipath are given at a 1.0% of time exceeded.
- In above calculation, we did not include the effects of propagation due to the roadside tree, vegetation, building, etc.
- In above calculation, we did not consider the effect of the system noise temperature increase due to the atmospheric attenuation. At low elevation angles this probably cannot be ignored. For example, the atmospheric background temperature can increase from 26K at 5° elevation angle to 70K at 1° elevation angle.

Table 6. Radio-Climatic Parameters at Wallops

Radio Parameters	February	May	August	November	Year average
Refractive Index	310 N-units		360 N-units		335 N-units
Refractivity Gradient	40 N-units		50 N-units		45 N-units
Percentage of time when Refractivity Gradient <-100N/km	4%	10%	15%	7%	9%
Water Vapor Content	5 g/m^3		12.0 g/m^3		8.5 g/m^3
Rainfall Rate 1.0% of Time					2.5 mm/h
Cloud Liquid Water Columnar Content 1.0% of Time					1.2 kg/m^2
Radio Climatic Zone					A1
Faraday Rotation					20°

Modeling the tail-end of spacecraft antenna patterns during spacecraft roll uncertainty

The Orion-Ares trajectory and attitude during launch and ascent are highly dynamic. The Ares System Requirement Document (SRD) indicates that during launch and ascent, Ares can experience a roll error of up to 10^o. In the vicinity of MECO and Separation, which occurs between Launch + 550 seconds and Launch + 650 seconds, the Wallops 11.3 m antenna is looking at the tail part of the DV and DFI antenna patterns, which have many fringes and are sensitive to roll angle error. Figure 11 and Figure 12 show the trajectory overlays onto the DV antenna pattern and onto the DFI antenna pattern for trajectories TD7-E, F, and G respectively. For example in Figure 1c, the DV antenna gain profile for trajectory TD7-F fluctuates erratically between -8 and -18 dB during the time window of Separation. Thus we need to use the worst antenna gain number within $+10^o$ and -10^o roll angle error for the low elevation link analysis of the DV and DFI links

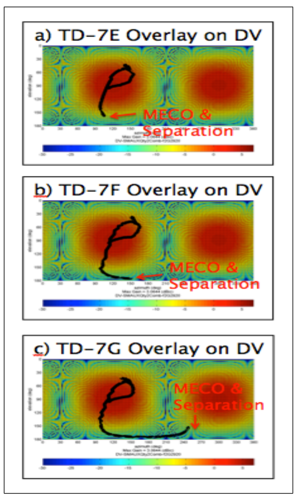

Figure 11 - Trajectory Overlay on DV Antenna Pattern

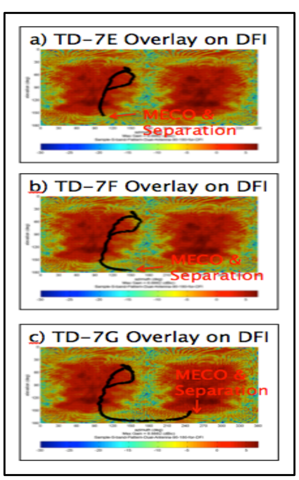

Figure 12 - Trajectory Overlay on DFI Antenna Pattern

Use of apparent angle instead of true angle at low elevation angle

Due to the existence of the atmospheric refractive index gradient (usually in the vertical direction), a radio beam ray emitted from a spacecraft would be bent towards to the Earth with a curvature as show in the figure. Thus the apparent elevation angle (θ) of a spacecraft is different from its true elevation angle (θ_0) (here the true angle is the elevation angle of the spacecraft under free space condition). This difference becomes significant at low elevation angles.

The apparent elevation angle is usually larger than the true elevation angle of the spacecraft relative to the ground receiving station as showed in Figure 13, and is expressed in the following equation:

$$\theta = \theta_0 + \tau_s(h, \theta_0) \text{ [degrees]} \qquad (6)$$

where τ_s is a diffraction correction term and is a function of the height (in km) and true elevation angle for the spacecraft. This term rapidly increases with decreasing elevation angle. For example, for a region with temperate maritime air, at 20° elevation angle, this deviation is 0.06°, while at 2° elevation angle, it becomes as large as 0.38°.

Thus, when we calculate the propagation loss, for this low elevation angle study, we should use the apparent elevation angle instead of the true elevation angle, because the apparent angle is the angle of radio ray path.

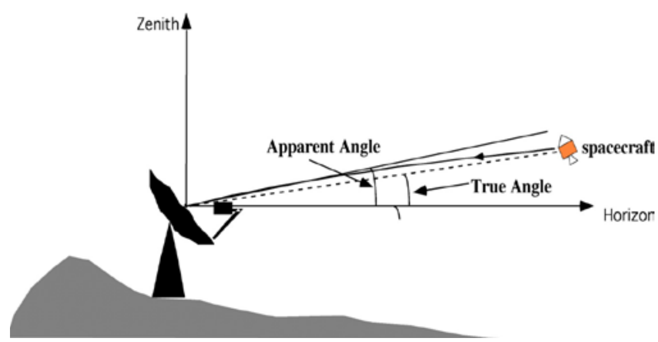

Figure 13 - shows the scenario of apparent angle and true angle for a spacecraft transmitting the signal at low elevation angles

5. Brief Description of Follow-on Work

ITU-R model theoretical results – proposed Recommendation ITU-R P.618 enhancement

Recommendation ITU-R 618.10 identifies several scintillation loss models depending on the level of fadings and elevation angles. The normal scintillation model is recommended for elevation angles of four degrees and higher. For lower elevation angles, the scintillation is decomposed into three parts; the deep, the shallow, and the asymptotic fadings. These models describe the percentage of time for which the scintillation loss exceeds certain loss. For losses of 25 dB or above the deep fading model is used. Based on this model, one can find the smallest possible percentage for which the scintillation loss is at 25 dB. Such point serves as the beginning and the peak of the shallow fading model. At the other end, the shallow scintillation attains the value of the asymptotic model, namely at percentage 63. For the percentages in between, the shallow model assumes a complicated highly nonlinear exponential model that interpolates the deep fading model and the asymptotic model. When implementing the ITU recommendations for the scintillation at Wallops, several inconsistencies were identified. First there is a mismatch in fading losses between the low and high elevation angles. Even worse, at times, the scintillation losses are larger at higher elevation angles. Most importantly, the interpolating model for the shallow model is so complex that its solution does not exist in several cases.

We propose a new shallow fading model to augment the existing ITU-R P.618 to guarantee (i) the existence of solution, (ii) the continuity of the fading models between low and high elevation angles, and (iii) the fadings decrease as the elevation angle increases. The proposed model will be validated with ITU-R low-elevation fading data and the Space Shuttle data.

Extraction of scintillation loss from WFF AGC and received power measurements STS-126, 127, 128, 129, and 130:

Wallops island tracking station routinely tracks Space Shuttle flights when they are launched from Florida launch site. The initial tracking is usually done by an antenna at the shuttle launch pad and also by the close by PDL tracking station so that the signal radiated by the shuttle as well as commanding signal impediment due to the shuttle engine plume can be mitigated. As soon as the shuttle reaches an altitude when it can be seen (line of sight) by the Wallops station, tracking is then taken over by the Wallops station and the tracking is continued till the shuttle disappears over the north-eastern horizon. Thus the Wallops station antenna goes through a low elevation angle scenario two times, once when the shuttle is rising and once when the shuttle is setting. Along with tracking the shuttle the station also routinely records the data received from the shuttle, one of the records is called the “Strip Chart” that records the signal power received by the station from the shuttle radiated signal. In this manner the shuttle fights 126, 127, 128, 129, and 130 were tracked by the Wallops station recently and the strip chart data are available.

The strip charts measure the power incident at the input to the Low Noise Amplifier (LNA) also known as the pre-amplifier using the AGC. The Wallops 11.3 m diameter antenna routinely used for tracking the shuttle splits the arriving downlink signal into the Right Hand Circular Polarization (RHCP) and Left Hand Circular Polarization (LHCP) components and in perfect operating conditions this incurs a 3 dB loss from the received signal power level. Each polarized component is then dealt with independently of the other. There is an AGC for each component circuit, AGC1 for RHCP and AGC2 for LHCP, and data of signal strength received for each component is recorded separately. Each track begins with a pre-calibration session and ends with a post-calibration session. The pre-calibration is performed when the antenna is at the horizon while the post-calibration is done with the antenna pointed at the zenith. In the calibration session, with no shuttle signal coming in, steps of voltages are input to the antenna horn that produce specific measured levels of power at the input to the pre-amplifier in the AGC1 and AGC2 respectively. The measured power levels to the pre-amplifier are plotted on the strip chart paper, the calibrations have a 5 dB step. To identify all the power level steps, the step that produces -90 dBm power level input to the pre-amplifier is made the longest in all the steps. Thus the calibration levels go from -70 dBm, -75 dBm, -80 dBm, -85 dBm, -90 dBm, -95 dBm, -100 dBm, -105 dBm, -110 dBm, -115 dBm, -120 dBm, -125 dBm with the -90 dBm step being the longest in time. Figure 14 shows the calibration steps.

After the pre-calibration is done the shuttle tracking may begin. The power level input to the pre-amplifier is measured for the shuttle signal received signal for AGC1 as well as AGC2 and a line chart is plotted on the strip chart paper. The actual power received from the shuttle signal for the RHCP or the LHCP component can then be obtained by a comparison of the calibration level steps. These levels were calculated and Figure 15 shows the results.

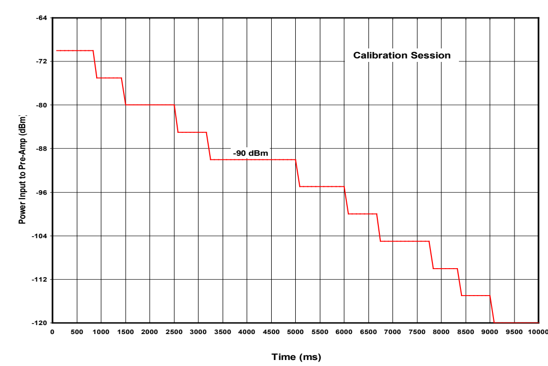

Figure 14 - Calibration levels for AGC1 and AGC2

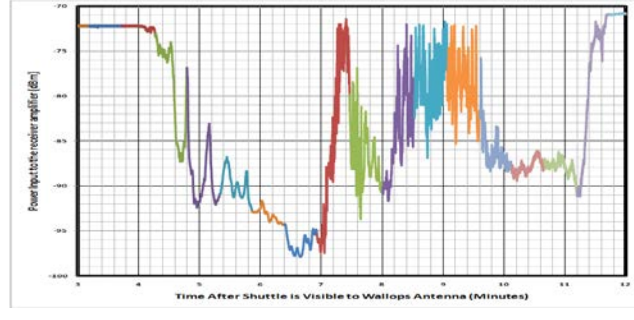

Figure 15 – Power received from the shuttle at Wallops

ground station

Support Flight Test 4 (Orion 2) Study

In February 2010, based on the findings of the Augustine Commission [13], President Barack Obama announced a proposal to cancel the Constellation Program starting with the 2011 fiscal year budget. He later announced changes to the proposal in a major space policy speech in April 2010, that the Constellation Program was to be redirected to modify the Orion spacecraft from its original purpose as a crewed spacecraft for flights to the ISS and the Moon into an emergency escape capsule for the ISS. Based on this redirection, a new flight test program with scaled down Orion design is currently being developed. The new Orion emergency capsule does not carry DV link, but its launch vehicle still retains a 20 Mbps DFI link. To ensure that SCaN can support the new Orion's flight tests, we re-ran the Wallops low elevation link analysis with the new DFI link parameters and trajectories, and the result is shown in Figure 16. Figure 16 indicates that the link margin is more than 10 dB for the DFI link in the vicinity of MECO and Separation. The reasons for this high link margin are:

(1) The new Orion's launch vehicle has a DFI passive loss of 1 dB, whereas the original Ares passive loss of 5.88 dB.

(2) With the new Orion's launch trajectory, MECO and Separation occur between 4^o and 7^o elevation angle, which is high enough so that the high scintillation loss does not kick in. In the previous TD7 launch trajectories, MECO and Separation occur between 2^o and 5^o elevation angle, thus causing high scintillation loss.

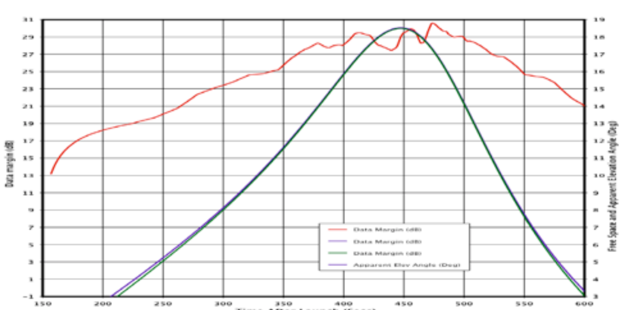

Figure 16

6. Concluding Remarks

In this paper, we discussed the challenges of the low elevation link analysis of the Orion-Ares launch and ascent links. The analysis techniques developed and the experience gained can be useful for future flight missions.

We identified the idiosyncrasies of the Recommendation ITU-R P.618 tropospheric models, and this lead to ongoing collaboration between the NASA SCaN Team and the US SG3 Team to refine and to advance the tropospheric scintillation modeling. We proposed a new approach to modeling the shallow fading within Recommendation ITU-R 618.10 while preserving the formulations for the ITU-R Deep and Normal fading. Our enhancement to the approach secures the existence of solution, removes the discontinuity between the models in the existing recommendations, and ensures that fading decreases as the elevation angle increases. We plan to acquire the ITU-R low-elevation fading data and the Space Shuttle data measured at Wallops to validate our proposed model.

Acknowledgement

This work was carried out at the Jet Propulsion Laboratory, California Institute of Technology, under a contract with the National Aeronautics and Space Administration. The research was supported by the NASA's Space Communication and Navigation (SCaN) Program.

References

[1] Ulaby, F. T., et al, *Microwave Remote Sensing, Active and Passive*, Vol. 1, Addison-Wesley Publishing Co., Reading, MA, 1981.

[2] DSMS Telecommunications Link Design Handbook, Document 810-005, Module 105 (Atmospheric and Environmental Effects), Jet Propulsion Laboratory, California Institute of Technology, Pasadena, CA, May 26, 2006.http://eis.jpl.nasa.gov/deepspace/dsndocs/810-005/

[3] S. D. Slobin, "Microwave noise temperature and attenuation of clouds: Statistics of these effects at various sites in the United States, Alaska, and Hawaii", *Radio Science*, vol. 17, no. 6, pp. 1443–1454, November–December 1982.

[4] Anil V. Kantak, "Satellite Communications" JPL Document, JPL D-32933.

[5] Anil V. Kantak and Stephan D. Slobin, "Atmosphere Attenuation and Noise Temperature Models at DSN Locations for 1 – 45 GHz" JPL Publication 09-14.

[6] ITU-R, Rec. P.618-10, Propagation data and prediction methods required for the design of Earth-space telecommunication systems, International Telecommunication Union, Geneva, 2009.

[7] ITU-R, Rec. P.453-9, The radio refractive index: its formula and refractivity data, International Telecommunication Union, Geneva, 2003.

[8] ITU-R, Rec. P.834-6, Effects of tropospheric refraction on radiowave propagation, International Telecommunication Union, Geneva, 2003.

[9] ITU-R, Rec. P.836, Water vapor: Surface density and total columnar content, International Telecommunication Union, Geneva, 2003.

[10] ITU-R, Rec. P.838, Specific attenuation model for rain for use in prediction methods, International Telecommunication Union, Geneva, 2003.

[11] ITU-R, Rec. P.676-4, Attenuation by Atmospheric Gases, International Telecommunication Union, Geneva, 1999.

[12] ITU-R, Rec. P.840-3, Attenuation due to clouds and fog, International Telecommunication Union, Geneva, 1999.

[13] Review of U.S. Human Spaceflight Plans Committee "Seeking a Human Spaceflight Program Worthy of a Great Nation," October 2009 http://legislative.nasa.gov/396093main_HSF_Cmte_FinalReport.pdf

BIOGRAPHY

Kar-Ming Cheung *is a Principal Engineer and a Technical Group Supervisor in the Communications Architecture and Research Section at JPL. His group supports communications and network architecture studies, and develops the analysis, modeling, and simulation*

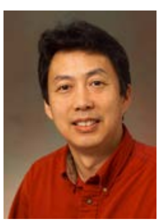

Christian Ho *is a senior telecommunications system engineer at the Jet Propulsion Laboratory. He is also an expert in the radio wave propagation in various environments (ionized and non-ionized media). He received his PhD in Space Physics from UCLA and joined JPL in 1993. He has more than 100 publications in a wide variety of fields, including radio wave propagation in the Earth's atmosphere, ionosphere, magnetosphere, solar corona and interplanetary medium; atmospheric reentry at Venus and Mars; interference in terrestrial environments; frequency selection for many NASA deep space missions, Deep Space Network interference protection; He is an expert in ITU (International Telecommunication Union) regulations and spectrum coordination, and he has made many contributions in drafting recommendations and issues for ITU.R Working Group.*

Anil V. Kantak *received the MSEE and the Ph.D. degrees from the University of Southern California. He has been with the Jet Propulsion Laboratory (JPL) since 1983, working on many engineering and scientific projects such as Voyager, Galileo, and Cassini missions. He has worked*

tools. He received NASA's Exceptional Service Medal for his work on Galileo's onboard image compression scheme. Since 1987 he has been with JPL where he is involved in research, development, production, operation, and management of advanced channel coding, source coding, synchronization, image restoration, and link analysis schemes. He got his B.S.E.E. degree from the University of Michigan, Ann Arbor in 1984, his M.S. degree and Ph.D. degree from California Institute of Technology in 1985 and 1987 respectively.

Dr. Charles H. Lee *is an associate professor of mathematics at the California State University Fullerton (CSUF) and a faculty part time staff in the Communications Architectures & Research Section (332) at the Jet Propulsion Laboratory. He received his Doctor of Philosophy in Applied Mathematics in 1996 from the University of California at Irvine. Before becoming a faculty member, he spent three years as a Post-Doctorate fellow at the Center for Research in Scientific Computation, Raleigh, North Carolina, where he was the recipient of the 1997-1999 National Science Foundation Industrial Post-Doctorate Fellowship. His research has been Computational Applied Mathematics with emphases in Control, Fluid Dynamics, Smart Material Structures, Telecommunications, and Biomedical Engineering. He has published over 12 mathematical and engineering journal articles and over 25 conference proceedings. In 2002, Dr. Lee received the Outstanding Paper Award from the International Congress on Biological and Medical Engineering.*

with the DSN for more than twenty five years analyzing and providing solutions for telecom systems problems for many missions tracked by DSN. He has published more than 35 publications including a book on satellite communications. He is the author of the CCSDS design control table used by the CCSDS community throughout the world.

Robert Tye *has been the National Aeronautics and Space Administration (NASA) Near Earth Network (NEN) lead responsible for the design and development of ground station support to the Constellation Program, the successor to NASA's Space Shuttle Program since January 2009. Prior to 2009, he spent 20 years with the* National Oceanic and Atmospheric Administration *(*NOAA*) in Silver Spring, Maryland, and Wallops, Virginia. While with NOAA, Rob held a number of positions from System Communication Engineer, where he designed, developed, and evaluated communication networks, computer systems, antenna systems, RF systems, satellite to ground station interfaces, and telemetry and command systems for the Geostationary Operational Environmental Satellite (GOES) and Polar Operational Environmental Satellite (POES) missions to Manager of the Wallops Computer Data Acquisition (CDA) System Planning and Development Branch (SP&D), where he provided the technical management of NOAA Wallops Command and Data Acquisition Station (WCDAS) and acted as lead engineer on major upgrades to prepare the* *station for the next generation of weather satellites. Rob began his career in 1984 as a Radio Frequency Engineer for Pan American Aerospace, where he designed, developed, and built space/ground based communication systems in support both crewed and uncrewed vehicles launching from Cape Canaveral, Florida. He holds a Bachelor's Degree in Electrical Engineering, with a Computer Science Minor, from Old Dominion University in Norfolk, Virginia, and a Master's Degree in Electrical Engineering from the Florida Institute of Technology in Melbourne, Florida.*

Catherine C. Sham joined NASA full time in May, *1987 as a radio frequency (RF) communications engineer in the Johnson Space Center (JSC) Engineering Directorate Communications & Tracking Division. Ms. Sham currently serves as the Chief of the Systems Planning, Analysis & Evaluation Branch and as the Center Spectrum Manager of the NASA/JSC in Houston, TX. Ms. Sham directs, manages, and mentors a team that is responsible for end-to-end avionics systems architecture, requirements & verification engineering, systems analysis & integration of JSC avionics products and external avionics interfaces with non-Program infrastructures. She is recognized as an expert in both regulatory and analytical aspect of Spectrum Management in NASA, domestic and international regulatory agencies, International Partner agencies and private enterprises. As the JSC Center Spectrum Manager, she is responsible for spectrum management for NASA's Manned Spaceflight Programs and the overall frequency compatibility of JSC through development, implementation of policies and applicable procedures and performing spectrum engineering & management functions. Ms. Sham graduated from Rice University in 1987 with a Bachelor of Science Degree in Electrical Engineering and a Bachelor of Arts in Mathematical Science. She also holds a Masters Degree in Electrical Engineering from Rice University (1989).*